LBNL-60247
Preprint


ERNEST ORLANDO LAWRENCE
BERKELEY NATIONAL LABORATORY

# Title: The Methanosarcina barkeri genome: comparative analysis with Methanosarcina acetivorans and Methanosarcina mazei reveals extensive rearrangement within methanosarcinal genomes

Author(s): Dennis L. Maeder, Iain Anderson, et al

Division: Genomics

November 2006

Journal of Bacteriology

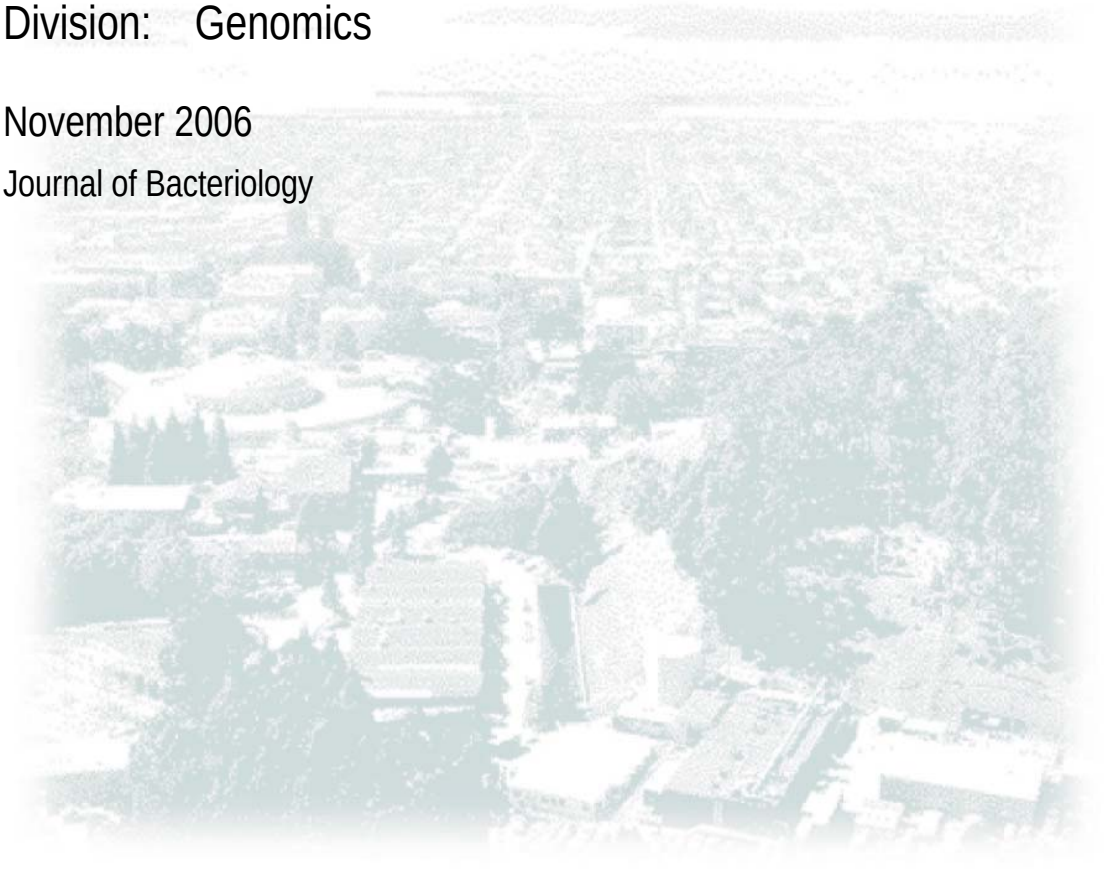

# The *Methanosarcina barkeri* genome: comparative analysis with *Methanosarcina acetivorans* and *Methanosarcina mazei* reveals extensive rearrangement within methanosarcinal genomes

Dennis L. Maeder*, Iain Anderson†, Thomas S. Brettin†, David C. Bruce†, Paul Gilna†, Cliff S. Han†, Alla Lapidus†, William W. Metcalf‡, Elizabeth Saunders†, Roxanne Tapia†, and Kevin R. Sowers*.

* *University of Maryland Biotechnology Institute, Center of Marine Biotechnology, Columbus Center, Suite 236, 701 E. Pratt St., Baltimore, Maryland 21202, USA*

† *Microbial Genomics, DOE Joint Genome Institute, 2800 Mitchell Drive, B400, Walnut Creek, CA 94598, USA*

‡ *University of Illinois, Department of Microbiology, B103 Chemical and Life Sciences Laboratory, 601 S. Goodwin Avenue, Urbana, Illinois 61801, USA*

Running title: Comparative analysis of three methanosarcinal genomes

Keywords: *Methanosarcina barkeri*, archaeal genome, methanogenic Archaea

# ABSTRACT

We report here a comparative analysis of the genome sequence of *Methanosarcina barkeri* with those *of Methanosarcina acetivorans* and *Methanosarcina mazei*. All three genomes share a conserved double origin of replication and many gene clusters. *M. barkeri* is distinguished by having an organization that is well conserved with respect to the other *Methanosarcinae* in the region proximal to the origin of replication with interspecies gene similarities as high as 95%. However it is disordered and marked by increased transposase frequency and decreased gene synteny and gene density in the proximal semi-genome. Of the 3680 open reading frames in *M. barkeri*, 678 had paralogs with better than 80% similarity to both *M. acetivorans* and *M. mazei* while 128 nonhypothetical orfs were unique (non-paralogous) amongst these species including a complete formate dehydrogenase operon, two genes required for N-acetylmuramic acid synthesis, a 14 gene gas vesicle cluster and a bacterial P450-specific ferredoxin reductase cluster not previously observed or characterized in this genus. A cryptic 36 kbp plasmid sequence was detected in *M. barkeri* that contains an *orc*1 gene flanked by a presumptive origin of replication consisting of 38 tandem repeats of a 143 nt motif. Three-way comparison of these genomes reveals differing mechanisms for the accrual of changes. Elongation of the large *M. acetivorans* is the result of multiple gene-scale insertions and duplications uniformly distributed in that genome, while *M. barkeri* is characterized by localized inversions associated with the loss of gene content. In contrast, the relatively short *M. mazei* most closely approximates the ancestral organizational state.

# INTRODUCTION

Biological methanogenesis by the methane-producing Archaea has a significant role in the global carbon cycle. This process is one of several anaerobic degradative processes that complement aerobic degradation by utilizing alternative electron acceptors in habitats where $O_2$ is not available (Sowers 2004). The efficiency of this microbial process is directly dependent upon the interaction of three metabolically distinct groups of microorganisms: the fermentative and acetogenic Bacteria and the methanogenic Archaea. The methanogenic Archaea have two pivotal roles in methanogenic consortia (Lovley and Klug 1982). By consuming hydrogen for methanogenesis and effectively lowering its partial pressure by the process of inter-species hydrogen exchange, the methanogens provide a thermodynamically favorable environment for the fermentative and acetogenic species to utilize protons as electron acceptors. This interaction enables fermentors to conserve more energy by producing a more oxidized product, acetate, which is a substrate for methanogenesis. The second role of the methanogens is the dismutation of acetate, which accounts for 70% of the global methane produced by biological methane production. The net effect of inter-species hydrogen exchange is the diversion of protons to hydrogen and carbon to acetate, which ultimately yields methane and carbon dioxide via methanogenesis.

The genus *Methanosarcina* includes the most metabolically diverse species of methanogens. Whereas most methanogenic species grow by obligate $CO_2$ reduction with $H_2$, methyl reduction with $H_2$, aceticlastic dismutation of acetate or methylotrophic

68 catabolism of methanol, methylated amines, and dimethylsulfide, most *Methanosarcina*
69 spp. grow by all four catabolic pathways (Welander and Metcalf 2005).
70 *Methanosarcina acetivorans* was recently reported also to grow non-methanogenically
71 with CO (Rother and Metcalf 2004). In addition to their appetency for all known
72 methanogenic substrates most *Methanonsarcina* spp. can grow in a minimal mineral
73 medium and fix molecular nitrogen (Bomar and Knoll 1985; Lobo and Zinder 1988).
74 They also adapt to intracellular solute concentrations ranging from freshwater to three
75 times that found in seawater (Sowers 1995) by osmoregulatory mechanisms that enable
76 them to synthesize or accumulate osmoprotectants and modify their outer cell envelope
77 (Sowers et al. 1993). This metabolic diversity is reflected in the relatively large genome
78 sizes of *Methanosarcina acetivorans* (5.8 Mb) and *Methanosarcina mazei* (4.1 Mb)
79 genomes and the relatively large number of number of putative coding sequences,
80 4,524 and 3,371 respectively, compared with other methanogenic Archaea
81 (Deppenmeier et al. 2002; Galagan et al. 2002). The adaptive success of these species
82 is further evident by the occurrence of multiple orthologs in the genomes including
83 multiple catabolic methyltransferases and carbon monoxide dehydrogenases, all three
84 known types of nitrogenases, and all four known chaperoning systems (Conway de
85 Macario et al. 2003; Deppenmeier et al. 2002; Galagan et al. 2002).

86 *Methanosarcina barkeri* Fusaro was isolated from sediment from Lago del
87 Fusaro, a freshwater coastal lagoon west of Naples, Italy (Kandler and Hippe 1977).
88 This isolate utilizes all three catabolic pathways and exhibits a dichotomous
89 morphology. When grown on freshwater medium this species grows as large
90 multicelluar aggregates imbedded in a heteropolysaccharide matrix (Figure 1)

composed primarily of D-galactosamine and D-glucuronic acid, termed methanochondroitin (Kreisl and Kandler 1986), whereas in marine medium these species grow as individual cells surrounded only by an S-layer (Sowers 1995). This isolate has been one of the most frequently studied methanosarcinal strains for the physiology, biochemistry and bioenergetics of methanogenesis (Sowers 2004). The development of a tractable methanosarcinal gene transfer system has led to a number of recent reports on the mechanisms of methanogenesis using genetic approaches (Rother and Metcalf 2005).

Herein we describe the genome of *M. barkeri,* which represents the third methanosarcinal genome sequenced. In addition to comparison of the genome annotation, this is the first three-way analysis of the complete genomes of closely related species in the methanogenic *Euryarchaeota*. Results reveal extensive gene rearrangements in *M. barkeri* relative to *M. acetivorans* and *M. mazei* and high degree of conservation within the fragments providing insight into the mechanisms of structural modification and the functional organization of the methanosarcinal genome.

# MATERIALS AND METHODS

## Growth conditions

The source for *Methanosarcina barkeri* Fusaro (=DSM 804) was described previously (Metcalf et al. 1996). *M. barkeri* was grown in F-medium (Sowers 1995) with 0.1 M trimethylamine, Where described growth was tested with 0.1 M sodium formate or with a headspace of 200 kPa $H_2$-$CO_2$ (80:20) substituted for trimethylamine. Cultures

were incubated statically at 35 $^{o}$C in the dark. Growth was monitored by measuring the optical density at 550 nm with a Spectronic 21 and by measuring methanogenesis by gas chromatography as described previously (Sowers et al. 1993; Sowers and Ferry 1983).

## Genome sequencing, assembly and finishing

Genomic DNA was isolated from *M. barkeri* Fusaro as described previously (Boccazzi et al. 2000). The genome of *M. barkeri* was sequenced at the Joint Genome Institute (JGI) using a combination of 3 kb, 8 kb and 40 kb (fosmid) DNA libraries. All general aspects of library construction and sequencing performed at the JGI can be found at http://www.jgi.doe.gov/. Draft assemblies were based on 89216 total reads. All three libraries provided 13x coverage of the genome. The Phred/Phrap/Consed software package (http://www.phrap.com) was used for sequence assembly and quality assessment (Ewing and Green 1998; Ewing et al. 1998; Gordon et al. 1998). After the shotgun stage, reads were assembled with parallel phrap (High Performance Software, LLC). Possible mis-assemblies were corrected with Dupfinisher (unpublished, C. Han) or transposon bombing of bridging clones (Epicentre Biotechnologies, Madison, WI). Gaps between contigs were closed by editing in Consed, custom primer walk or PCR amplification (Roche Applied Science, Indianapolis, IN). A total of 2389 additional reactions were necessary to close gaps and to raise the quality of the finished sequence. The completed genome sequences of *M. barkeri* contains 85812 reads, achieving an average of 12-fold sequence coverage per base with an error rate less than 1 in 100,000. The sequences of *M. barkeri*, including a chromosome and a

plasmid, can be accessed using the GenBank accession numbers CP000099 and CP000098 or from the JGI IMG site (http://img.jgi.doe.gov) as taxon ID 623520000.

## Annotation and analysis

Genes were predicted with a combination of Glimmer and Critica (Badger and Olsen 1999; Delcher et al. 1999). These gene predictions were then run through a pipeline that identifies gene overlaps, missed genes, and incorrect start sites (Markowitz et al. 2006). The gene predictions were then manually curated. Functional predictions were generated automatically based on presence of hits to COGs (Tatusov et al. 2003), Pfam (Bateman et al. 2000), and Interpro (Mulder et al. 2005) families.

## Whole genome alignment and analysis

Chromosome sequences (Table 1) in fasta format were used to build single sequence blast databases, which served as the subject sequences for comprehensive WuBlast (Gish, W., 1996-2004, http://blast.wustl.edu) blastn and tblastx paired comparisons both as whole sequences and as segmented comparisons using the following parameters: span2, noseqs, filter=none, hspmax =10000, gspmax=10000. Similarly all CDS sequence features were built into databases and blasted to generate a comprehensive set of pairwise comparisons. Blastn outputs were captured into a database of HSP features cross referenced to a sequence and sequence feature database. Outputs were also directly parsed by Cross (Maeder, D., 1998-2006, http://bigm.umbi.umd.edu/materials/software/Cross.pub/) for display and interactive examination of comparative features.

The paired comparison database, GRIT, runs under the database manager MySQL (MySQL AB) and consists of source, feature, fragment and link tables. The feature table was populated with predicted gene product features derived from GenBank or JGI (Table 1) with a foreign key pointing to a source table. The link table contains blastn HSP scores and identities with foreign keys pointing to entries in the fragment table, which contains positional information about HSPs with a foreign key pointing to the feature from which it was derived. This schema (Figure 2) allows the construction of a SQL query that directly and rapidly retrieves sets of features, which are either unique within a set of source chromosomes or describes a set of genes common at an arbitrary level of similarity between two or more sources. Blastn comparisons facilitate measurement of significant similarity in homologs of closely related organisms and manage non-coding sequences; tblastx or blastx comparisons are similarly applicable for comparison of less closely related sequences. Washu blastn was used with the parameters: span2, filter=none, hspmax =10000, gspmax=10000, and was wrapped in a perl script for automatic iteration through multiple pair-wise blasts. Output data were then parsed and HSPs stored in GRIT. A web interface to the queries and databases is available at (http://bigm.umbi.umd.edu/dat/genome/) and will be elaborated elsewhere.

Cumulative skew analysis was performed using skew (Maeder, 2001, http://bigm.umbi.umd.edu/materials/software/skew/) which implements the algorithm of Grigoriev (Grigoriev 1998). Repeat analysis emerged directly from unfiltered blast and was confirmed using Mummer (Delcher et al. 1999). Putative origins of replication were

explored by examining regions with locally separated inverted repeats in close upstream proximity to the *orc1/cdc6* genes.

Chromosomal sequence similarity was calculated as a distance derived from blastn comparisons in the GRIT database using a perl script cross match.pl which generates distance matrices in mega2 format based on equation 1, where $n$ is the length of the genome and HSP.ID is the maximal fractional identity at position $n$ of sequence $x$ where HSP.ID exceeds a threshold of e.g. 0.67. The mean distance $D$ for both axes is calculated for both sequence axes by the equation:

$$D_x = 1 - \sum_1^n (MAX(HSP.ID_n))/n \quad (1)$$

This measure of distance is comparable with hybridization techniques as it yields a fractional nucleotide similarity between organisms which considers stringency.

Synteny of any gene was measured by comparing the order of the gene's left and right neighbors with those of their best matched paralogous genes in the comparable genome. Downstream synteny is expressed as the ratio of the ordinal distance between a gene, G, and it's downstream neighbor, R, (which is always 1) and the distance between a corresponding paralogous gene G' and the paralog of R, R'. This may be calculated as:

$$SI = 1/abs(R' - G') \quad (2)$$

with 0 < SI <= 1. Cumulative deviations from the mean of SI were calculated for intelligible display. Intergenic interval was calculated in the same manner.

198 ### Microscopy

199 For thin-section electron micrographs, cells were fixed with 2% glutaraldehyde
200 and 2% osmium tetroxide, and dehydrated in a graded series of ethanol mixtures. Cells
201 were embedded and sectioned in Epon resin, then post-stained with uranyl acetate and
202 lead citrate as described previously (Sowers and Ferry 1983). A Joel JEM-1200 EX II
203 transmission electron microscope at 80 kV was used to generate thin-section
204 micrographs.

205 # RESULTS & DISCUSSION

206
207
208 The genome of *Methanosarcina barkeri* was sequenced using a combination of
209 whole genome shotgun and directed finishing as described in Methods. The genome
210 consists of a circular chromosome of 4,837,408 base pairs (bp) and a 36,358 bp
211 extrachromosomal element (Table 1). The *M. barkeri* genome, which is intermediate in
212 size between *Methanosarcina acetivorans* (5.8 mb) and *Methanosarcina mazei* (4.1
213 mb), is the second largest genome among the Archaea. The extrachromosomal
214 element is 6.7 times larger than the only other methanosarcinal extrachromosomal
215 element, plasmid pC2A, from *M. acetivorans* (Metcalf et al. 1997).

216 ## *Methanosarcina barkeri* chromosome structure and content

217
218 A total of 3680 putative protein coding genes longer than 200 bp were identified
219 (Table 1), which together cover 70% of the genome. The average protein coding region
220 of *M. barkeri* at 921 bp is within 2% of *M. acetivorans* and *M. mazei* while its average
221 intergenic region at 393 bp is considerably larger than those of *M. acetivorans* (328 bp)

and *M. mazei* (303 bp). A further 73 RNA features were identified including 3 sets of ribosomal RNAs (5S, 16S, 23S) and 62 tRNAs covering all amino acids and pyrrolysine that is encoded by the UAG codon in methylamine methyltransferase genes. 1780 hypothetical protein open reading frames accounted for nearly half of all protein features with 1837 putative functional proteins assignments based on similarity to identified protein sequences in public databases. Of hypothetical protein genes conserved at the 80% nucleotide level, 289 were shared with *M. acetivorans* and 249 with *M. mazei* of which 105 were common to both and should be considered highly conserved unidentified genes.

## Gene Annotation

There were 128 unique orfs with sequence identities greater than 67% to genes in the NCBI sequence database but without sequence identity to other methanosarcinal genomes (http://bigm.umbi.umd.edu/materials/Methanosarcina/). Some of these features are highlighted below.

The *M. barkeri* genome included the full complement of genes encoding enzymes in the hydrogenotrophic, methylotrophic and aceticlastic pathways (Deppenmeier et al. 2002; Galagan et al. 2002). In addition to these a complete formate dehydrogenase operon (MbarA 1561-1562), *fdhAB*, was detected with high sequence identity to catabolic formate dehydrogenase from several formate-utilizing methanogens. *Methanosarcina* spp. have never been reported to utilize formate for growth and *fdhAB* has not been detected previously in this genus (Boone et al. 2001). Attempts to grow *M. barkeri* on 50 mM formate in this study were unsuccessful and the

addition of sodium formate to cultures containing trimethylamine or hydrogen did not enhance growth. *M. barkeri* lacks genes encoding a two subunit NDP-forming acetyl-CoA synthetase (*acd*AB) that is found in *M. acetivorans* (MA3168 and MA3602) and *M. mazei* (MM0358 and MM0493), but has a remnant of this enzyme, pseudogene MbarA_3662. This enzyme catalyzes one of two pathways for generating acetyl-CoA; the other is the CO dehydrogenase/acetyl-coenzyme A synthase that catalyzes aceticlastic catabolism in *Methanosarcina* spp. The absence of the *acd* genes suggests that the CO dehydrogenase/acetyl-coenzyme A synthase fulfills the function of both enzymes in *M. barkeri.*

Among genes encoding biosynthetic functions a group of 14 sequential orfs encode for predicted gas vesicles with highest identity to *Gvp*ANOFGJKLM (MbarA326-339) in the haloarchaea, which includes the minimal gene set for expression of vesicle in *Haloferax volcanii* (Offner and Pfeifer 1995). Although there are no reports of gas vesicles in *M. barkeri* Fusaro, gas vesicles have been reported in another strain of *M. barkeri*, FR-1, and in *Methanosarcina vacuolata*, which has 61% homology with the type strain of *M. barkeri* (Archer and King 1984; Zhilina and Zavarzin 1979; Zhilina and Zavarzin 1987). Interestingly, *M. barkeri* has three sequential copies of *Gvp*A that encodes the ribs of the vesicle wall and influences the strength and width of the vesicles (Beard et al. 2002). The 33.5 kb region that includes the *Gvp* operon may have been acquired from vesicle synthesizing species as it is flanked by transposons. Gas vesicles are observed occasionally in *M. barkeri* cells grown with $H_2$-$CO_2$ on solidified medium. *M. barkeri* also has orfs (MbarA_0022 and MbarA_0023) with high identity to two enzymes required for N-acetylmuramic acid synthesis, which is unique among the

sequenced Archaea. However, prior analysis of the cell wall compositon of *M. barkeri* Fusaro failed to detect muramic acid (Kandler and Hippe 1977). *M. barkeri* also lacks a low affinity phosphate transporter (MA2935) suggesting it originated in a phosphate-poor environment. Two other transporters are missing in *M. barkeri*, a gluconate transporter (MA0021) and a dicarboxylate transporter (MA2961). This suggests that *M. barkeri* may have a lower ability to take up organic compounds than the other two. Finally *M. acetivorans* and *M. mazei* have two copies of cheC (MA0012 and MA3065) but *M. barkeri* does not have this protein. The role of this chemotaxis gene in *Methanosarcina* spp. is currently unknown since motility has not been observed in these species.

Another unique feature of the *M. barkeri* genome is the detection of a putative operon encoding a bacterial P450-specific ferredoxin reductase (Mbar 1947-1945). The family of heme protein monooxygenases known as cytochrome P450 plays a critical role in the synthesis and degradation of many xenobiotics and physiologically important compounds (Sono et al. 1966; Sono et al. 1996; Whitlock and Denison 1995). All known P450s are multi-centre enzymes consisting of a heme, or P450, component with associated reductase components. The gene encoding the putative cytochrome P450 in *M. barkeri* is flanked immediately upstream by genes encoding a ferredoxin and ferredoxin reductase, which is typical of bacterial class I three-component systems. For catalytic activity, cytochrome P450 must be associated with the electron donor partner proteins, ferredoxin/ferredoxin reductase complex (Takemori et al. 1993). Cytochrome P450 has not been detected previously in the Archaea. Another putative operon encoding oxygen dependent cytochome *d* oxidase, *cydAB*, was also identified in the

genome of *M. barkeri* and the other two methanosarcinal genomes. The presence of these oxygen dependent genes along with one catalase and two superoxide dismutase suggests that these proteins protect methanosarcinal species from oxygen or they may support microaerophilic growth by a currently undescribed mechanism. As cytochrome P450 catalyzes an oxygen requiring reaction and has not been detected previously in an anaerobe, the detection of this gene in *M. barkeri* raises intriquing questions about the function of this gene product in this obligately anaerobic methanogen.

## Plasmid structure and content

The 36.4 kb plasmid in *M. barkeri* has not been detected previously. In contrast to the smaller 5.4 kb plasmid pC2A in *M. acetivorans*, which appears to replicate by a rolling-circle mechanism (Metcalf et al. 1997), the *M. barkeri* extrachromosomal element lacks a putative *rep*A. Instead it has a cdc-6 homolog in a region of highly repetitive sequence (discussed below), which suggests a novel mechanism of synchronous replication. Interestingly, one of the extrachromosomal orfs (MbarB 3749) has 44% sequence similarity to an ATPase associated with chromosomal partitioning. These combined characteristics suggest that the extrachromosomal element replicates with cell division. In addition to the putative cdc6 and partitioning protein, the orfs include 4 genes possibly associated with methanochondroitin synthesis, 7 hypothetical genes of unknown function and 5 putative transposases. None of the orfs had equivalent identities to orfs found in *M. acetivorans* and *M. mazei* genomes, but missing from the *M. barkeri* genome that might have suggested a critical function for the extrachromosomal element.

## Features revealed by whole genome comparison

Whole genome distances (Table 2) based on maximal local alignments indicate that the genomes are quite similar in overall content with *M. acetivorans* and *M. mazei* marginally more closely related. This is in qualitative agreement with DNA-DNA hybridization experiments (Sowers and Johnson 1984), which showed 28% homology between *M. acetivorans* and *M. mazei* and 18% between these species and *M. barkeri.* This result underscores the comparability of these sequences with the exception of the plasmid sequence.

## Location of origins of replication

In Archaea, origins of replication are invariably found in close proximity to the origin recognition complex gene (*orc1*) sometimes also referred to as cell division control protein 6 (*cdc6*) (Lopez et al. 1999). When genes are densely packed, searches for putative origins of replication are directed at proximal intergenic regions. In the three Methanosarcinae there are two highly conserved paralogous copies of these genes, in relatively close mutual proximity (about 100 kb or 300 kb in *M. barkeri*) situated on opposite strands and directed away from each other, a finding consistent with the observation of Kelman *et al.* (Kelmana and Kelman 2004). Flanking downstream ORFs are conserved (Table 3). The putative origins of replication are located in the upstream intergenic regions of approximately 1600 nt (ORI A) or 800 nt (ORI B) in extent and are somewhat conserved at the nucleotide level. In the chromosomal origin of replication region, gene products are approximately 95% identical across all species. Non-coding origin features (ORI A and ORI B) are not as well conserved (E <= 1e-44 in ORI A and

E <=1e-8 in ORI B) and show only weak similarity between ORI A and ORI B. They are extremely AT rich (~70%) and may show unconserved inverted repeat structures.

A replication complex is initiated when orc1 (cdc6) protein binds to cognate DNA at the origin and allows the recruitment of MCM and the rest of the replication machinery. An approximate inverted repeat (Figure 3) could allow a pseudo-symmetrical double hairpin to form a crucifix motif similar to a Holliday junction thereby initiating bi-directional replication from a point, with complexes bypassing each other to replicate the origin at the beginning of replication. The concurrent presence of more than one active origin would cause contention for DNA, so there must be an implicit mechanism to control which origin and which origin recognition complex protein is dominant. It is notable that the downstream neighbor of the secondary orc1 B is a highly conserved hsp60 class heatshock protein as this suggests a possible stress-associated switching mechanism. The putative origins of replication are located centrally within the most highly conserved and syntenous regions of the respective genomes (Figure 4) consistent with the observation of Eisen et al. (Eisen et al. 2000) of symmetrical inversion about the origin of replication. GC skew analysis (results not shown) is not useful in this case as there is a high level of strand inversion and rearrangement.

The plasmid of *M. barkeri* presents a unique and distinct origin of replication characterized by an orc1 homolog (orc1 C) that is relatively weakly related to orc1 A and orc1 B, (37% / 66% with orc1 A, 21% / 44% with orc1 B) (Table 3). The immediately adjacent upstream region of the plasmid DNA contains a 5.6 kb non-coding

region (15.3% of the plasmid sequence) characterized by highly repetitive sequence consisting of over 38 direct repeats of a 143 nt sequence with few variations between them (Figure S-1, supplement). The consensus of the AT rich repeat sequence is:

ATCCCATTTCCTAAGCAGAGAATTAGTTTCCTAAGCAAAAAAAAaGATTTCTGgcttagA
CCATTTCCTAAGCAAAACGATATCAGAAGACATAACAAGTTAGAAGAaAAAtAAgTT
AAAATTAGATATTAATCTGTATATAT, with internal repeats underscored and variable regions in lowercase. This sort of arrangement (ORI C) is quite unlike that of the chromosomal ORI A and ORI B, but has the capacity to present slideable bubbled-out complete repeat motifs and retain a quasi-stable structure (Figure 5).

**Overall genomic organization**

A significant observation in the three-way comparison of the Methanosarcina genomes (Figure 4) is the overall collinearity of *M. mazei* and *M. acetivorans* (lower left panel). This attests to a history of conserved gene order and resistance to large scale mosaicity. However closer examination (Figure 6) reveals that there is considerable deviation from the expected 45° slope for a line of identity. This is maintained between *M. barkeri* and *M. mazei*, indicating that *M. acetivorans* has been subject to uniformly distributed local elongation, which may arise from gene duplication, elongation of intergenic regions or insertion of sequence by transposition. This may explain the large size of the *M. acetivorans* genome relative to the other *Methanosarcina* spp.

*M. barkeri* is distinguished by having an organization that is well conserved with respect to the other *Methanosarcinae* in the region proximal to the origin of replication where interspecies gene similarities are as high as 95% (Table 3). However there is

383 little apparent conservation of gene organization in the region most distal to the origin
384 where large scale collinearity appears rare. The putative terminus of replication is
385 observed to be a hotspot for reorganization (Myllykallio et al. 2000). Two properties of
386 *M. barkeri* were measured: synteny, which measures the local paralog neighborhood
387 with respect to comparable genomes and intergenic interval or the separation between
388 successive genes which measures the relative content density. In the distal semi-
389 genome the rate of change of synteny is negative in accord with the macroscopic
390 observation of decreased collinearity, and the negatively correlated intergenic interval is
391 greater than average indicating a loss of gene content in this region (Table 2). What
392 might cause this wasteland effect? One possibility, given the symmetry with respect to
393 the origin, is an accumulation of strand exchange failures in the replication process, and
394 subsequent 'gene rot' of broken genes. The cross effect of random strand inversion
395 noted by Eisen et al. (Eisen et al. 2000) gives way to a shotgun effect. Another
396 possibility is infiltration by transposons with transposase mediated damage. Certainly
397 there is an increased frequency of transposon genes in this area (Figure 4, trace d), but
398 this may either be causative or opportunistic, with the organism tolerating infiltration of
399 already dysfunctional sections of the chromosome.
400

401 # CONCLUSIONS
402
403 Of the 3680 open reading frames in *M. barkeri*, 678 had paralogs with better than
404 80% similarity to both *M. acetivorans* and *M. mazei* while 256 were unique (non-
405 paralogous) amongst these species. An etiology for genome rearrangement is revealed
406 by whole genome comparison of three species of the genus *Methanosarcina*. The

inverse correlation of intergenic size and synteny demonstrates a mechanism for the development of genome plasticity, which involves replication associated inversion with concommitant gene damage and colonization by transposon elements. Gene duplication is also observed as a mechanism for genome extension. The organization of *M. barkeri* is well conserved with respect to the other *Methanosarcinae* in the region proximal to the origin of replication with interspecies gene similarities as high as 95%. In the half genome most distant from the origin, it is however disordered and marked by increased transposase frequency and decreased gene synteny and gene density. Furthermore we have observed a highly conserved double origin of replication which suggests a mechanism for replication which allows a double start with pass through which enables the origin itself to be replicated. The apparent genome plasticity likely contributed to these species ability to adapt to a broad range of environments as a result of genome elongation and enrichment for favorable phenotypes.

# ACKNOWLEDGEMENTS

This work was performed under the auspices of the US Department of Energy's Office of Science, Biological and Environmental Research Program and the by the University of California, Lawrence Livermore National Laboratory under Contract No. W-7405-Eng-48, Lawrence Berkeley National Laboratory under contract No. DE-AC03-76SF00098 and Los Alamos National Laboratory under contract No. W-7405-ENG-36. KRS was supported in part by NSF MCB Division of Cellular and Bioscience grant #MCB0110762 and by DOE Energy Biosciences Program grant #DE-FG02-93-ER20106. WWM was supported in part by NSF MCB Division of Cellular and Biosciences grant #MCB12466 and by DOE Energy Biosciences Program grant # DEFG02-02ER15296.

# LITERATURE CITED

Archer, D.B. and N.R. King. 1984. Isolation of gas vesicles from Methanosarcina barkeri. *J. Gen. Microbiol.* **130:** 167-172.

Badger, J.H. and G.J. Olsen. 1999. CRITICA: Coding Region Identification Tool Invoking Comparative Analysis. *Mol. Biol. Evol.* **16:** 512–524.

Bateman, A., E. Birney, R. Durbin, S.R. Eddy, K.L. Howe, and E.L. Sonnhammer. 2000. The Pfam protein families database. *Nucleic Acids Research* **28:** 263-266.

Beard, S.J., P.K. Hayes, F. Pfeifer, and A.E. Walsby. 2002. The sequence of the major gas vesicle protein, GvpA, influences the width and strength of halobacterial gas vesicles. *FEMS Microbiol. Lett.* **213:** 149-157.

Boccazzi, P., K.J. Zhang, and W.W. Metcalf. 2000. Generation of dominant selectable markers for resistance to pseudomonic acid by cloning and mutagenesis of the *ileS* gene from the archaeon *Methanosarcina barkeri* Fusaro. *J. Bacteriol.* **182:** 2611-2618.

Bomar, M. and K.W. Knoll, F. 1985. Fixation of molecular nitrogen by methanosarcina barkeri. *FEMS Microbiol. Ecol.* **31:** 47-55.

Boone, D.R., W.B. Whitman, and Y. Koga. 2001. Genus *Methanosarcina*. In *Bergey's Manual of Systematic Bacteriology* (eds. D.R. Boone and R.W. Castenholz), pp. 268-276. Springer, New York.

Conway de Macario, E., D.L. Maeder, and A.J.L. Macario. 2003. Breaking the mould: archaea with all four chaperoning systems. *Biochemical and Biophysical Research Communications* **301:** 811-812.

457 Delcher, A.L., D. Harmon, S. Kasif, O. White, and S.L. Salzberg. 1999. Improved
458 microbial gene identification with GLIMMER. *Nucleic Acids Research* **27:** 4636-
459 4641.
460 Deppenmeier, U., A. Johann, T. Hartsch, R. Merkl, R.A. Schmitz, R. Martinez-Arias, A.
461 Henne, A. Wiezer, S. Bäumer, C. Jacobi, H. Brüggemann, T. Lienard, A.
462 Christmann, M. Bömeke, S. Steckel, A. Bhattacharyya, A. Lykidis, R. Overbeek,
463 H.-P. Klenk, R.P. Gunsalus, H.J. Fritz, and G. Gottschalk. 2002. The genome of
464 *Methanosarcina mazei:* Evidence for lateral gene transfer between Bacteria and
465 Archaea. *J. Mol. Microbiol. Biotechnol.* **4:** 453-461.
466 Eisen, J., J. Heidelberg, O. White, and S. Salzberg. 2000. Evidence for symmetric
467 chromosomal inversions around the replication origin in bacteria. In *Genome*
468 *Biology*, pp. RESEARCH0011.
469 Ewing, B. and P. Green. 1998. Base-calling of automated sequencer traces using
470 phred. II. Error probabilities. *Genome Research* **8:** 186-194.
471 Ewing, B., L. Hillier, M.C. Wendl, and P. Green. 1998. Base-calling of automated
472 sequencer traces using phred. I. Accuracy assessment. *Genome Research* **8:**
473 175-185.
474 Galagan, J.E., C. Nusbaum, A. Roy, M.G. Endrizzi, P. Macdonald, W. FitzHugh, S.
475 Calvo, R. Engels, S. Smirnov, D. Atnoor, A. Brown, N. Allen, J. Naylor, N.
476 Stange-Thomann, K. DeArellano, R. Johnson, L. Linton, P. McEwan, K.
477 McKernan, J. Talamas, A. Tirrell, W.J. Ye, A. Zimmer, R.D. Barber, I. Cann, D.E.
478 Graham, D.A. Grahame, A.M. Guss, R. Hedderich, C. Ingram-Smith, H.C.
479 Kuettner, J.A. Krzycki, J.A. Leigh, W.X. Li, J.F. Liu, B. Mukhopadhyay, J.N.

480 Reeve, K. Smith, T.A. Springer, L.A. Umayam, O. White, R.H. White, E.C. de
481 Macario, J.G. Ferry, K.F. Jarrell, H. Jing, A.J.L. Macario, I. Paulsen, M. Pritchett,
482 K.R. Sowers, R.V. Swanson, S.H. Zinder, E. Lander, W.W. Metcalf, and B.
483 Birren. 2002. The genome of *Methanosarcina acetivorans* reveals extensive
484 metabolic and physiological diversity. *Genome Research* **12:** 532-542.
485 Gordon, D., C. Abajian, and P. Green. 1998. Consed: a graphical tool for sequence
486 finishing. *Genome Research* **8:** 195-202.
487 Grigoriev, A. 1998. Analyzing genomes with cumulative skew diagrams. *Nucleic Acids*
488 *Research* **26:** 2286–2290. .
489 Kandler, O. and H. Hippe. 1977. Lack of peptidoglycan in the cell walls of
490 Methanosarcina barkeri. *Arch. Microbiol.* **113:** 57-60.
491 Kelmana, L.M. and Z. Kelman. 2004. Multiple origins of replication in archaea *Trends in*
492 *Microbiology* **12** 399-430.
493 Kreisl, P. and O. Kandler. 1986. Chemical structure of the cell wall polymer
494 methanosarcina. *Syst. Appl. Microbiol.* **7:** 293-299.
495 Lobo, A.L. and S.H. Zinder. 1988. Diazotrophy and Nitrogenase Activity in the
496 Archaebacterium Methanosarcina barkeri 227. *Appl. Environ. Microbiol.* **54:**
497 1656-1661.
498 Lopez, P., H. Philippe, H. Myllykallio, and P. Forterre. 1999. Identification of putative
499 chromosomal origins of replication in Archaea. *Molecular Microbiology* **32:** 883-
500 886.
501 Lovley, D.R. and M.J. Klug. 1982. Intermediary metabolism of organic matter in the
502 sediments of a eutrophic lake. *Appl. Environ. Microbiol.* **43:** 552-560.

503 Markowitz, V., F. Korzeniewski, K. Palaniappan, E. Szeto, G. Werner, A. Padki, X.
504 Zhao, I. Dubchak, P. Hugenholtz, I. Anderson, A. Lykidis, K. Mavromatis, N.
505 Ivanova, and N.C. Kyrpides. 2006. The Integrated Microbial Genomes (IMG)
506 System. *Nucleic Acids Research (special database issue)* **34:** D344-348.
507 Metcalf, W.W., J.K. Zhang, E. Apolinario, K.R. Sowers, and R.S. Wolfe. 1997. A genetic
508 system for Archaea of the genus *Methanosarcina*: Liposome-mediated
509 transformation and construction of shuttle vectors. *Proc Natl Acad Sci USA* **94:**
510 2626-2631.
511 Metcalf, W.W., J.K. Zhang, X. Shi, and R.S. Wolfe. 1996. Molecular, genetic, and
512 biochemical characterization of the serC gene of Methanosarcina barkeri fusaro.
513 *J Bacteriol* **178:** 5797-5802.
514 Mulder, N.J., R. Apweiler, T.K. Attwood, A. Bairoch, A. Bateman, D. Binns, P. Bradley,
515 P. Bork, P. Bucher, L. Cerutti, and e. al. 2005. InterPro, progress and status in
516 2005. *Nucleic Acids Research* **33:** D201–D205.
517 Myllykallio, H., P. Lopez, P. Lopez-Garcia, R. Heilig, W. Saurin, Y. Zivanovic, H.
518 Philippe, and P. Forterre. 2000. Bacterial Mode of Replication with Eukaryotic-
519 Like Machinery in a Hyperthermophilic Archaeon. *Science* **288:** 2212-2215.
520 Offner, S. and F. Pfeifer. 1995. Complementation studies with the gas vesicle-encoding
521 p-vac region of Halobacterium salinarium PHH1 reveal a regulatory role for the
522 p-gvpDE genes. *Mol. Microbiol.* **16:** 9-19.
523 Rother, M. and W.W. Metcalf. 2004. Anaerobic growth of Methanosarcina acetivorans
524 C2A on carbon monoxide: An unusual way of life for a methanogenic archaeon.

*Proceedings of the National Academy of Sciences of the United States of America* **101:** 16929-16934.

Rother, M. and W.W. Metcalf. 2005. Genetic technologies for Archaea. *Curr Opin Microbiol* **8:** 745-751.

Sono, M., M.P. Roach, E.D. Coulter, and J.H. Dawson. 1966. *Chem.Rev.* **96:** 2841-2887.

Sono, M., M.P. Roach, E.D. Coulter, and J.H. Dawson. 1996. Heme-containing oxygenases. *Chem. Rev.* **96:** 2841-2887.

Sowers, K.R. 1995. Growth of *Methanosarcina* spp. as single cells. In *Archaea: A Laboratory Manual* (eds. F.T. Robb K.R. Sowers S. DasSharma A.R. Place H.J. Schreier, and E.M. Fleischmann), pp. 61-62. Cold Spring Harbor Laboratory Press, Cold Spring Harbor.

Sowers, K.R. 2004. Methanogenesis. In *The Desk Encylopedia of Microbiology* (ed. M. Schaechter), pp. 659-679. Elsevier Academic Press, San Diego.

Sowers, K.R., J.E. Boone, and R.P. Gunsalus. 1993. Disaggregation of *Methanosarcina* spp. and growth as single cells at elevated osmolarity. *Appl. Environ. Microbiol.* **59:** 3832-3839.

Sowers, K.R. and J.G. Ferry. 1983. Isolation and characterization of a methylotrophic marine methanogen, Methanococcoides methylutens gen. nov., sp. nov. *Appl. Environ. Microbiol.* **45:** 684-690.

Sowers, K.R. and J.L.F. Johnson, J. G. 1984. Phylogenetic relationships among the methylotrophic methane-producing bacteria and emendation of the familyMethanosarcinaceae. *Int. J. Syst. Bacteriol.* **34:** 444-450.

548 Takemori, S., T. Yamazaki, and S. Ikushiro. 1993. Evolution and differentiation of P450
549 genes. In *Cytochrome P450* (ed. T. Omura, Ishimura, Y., and Fujii-Kuriyama, Y.).
550 VCH Publishers, Inc., New York.
551 Tatusov, R.L., N.D. Fedorova, J.D. Jackson, A.R. Jacobs, B. Kiryutin, E.V. Koonin, D.M.
552 Krylov, R. Mazumder, S.L. Mekhedov, A.N. Nikolskaya, and e. al. 2003. The
553 COG database: an updated version includes eukaryotes. *BMC Bioinformatics* **4:**
554 41.
555 Welander, P.V. and W.W. Metcalf. 2005. Loss of the mtr operon in Methanosarcina
556 blocks growth on methanol, but not methanogenesis, and reveals an unknown
557 methanogenic pathway. *PNAS* **102:** 10664-10669.
558 Whitlock, J.P.J. and M.S. Denison. 1995. In dusction of cytochrome P450 enzyme that
559 metabolize xenobiotics. In *Cytochrome P450: Structure, Mechanisms and*
560 *Biochemistry* (ed. P.R. Ortiz de Montellano), pp. 367-390. Plenum Press, New
561 York.
562 Zhilina, T.N. and G.A. Zavarzin. 1979. Comparative cytology of methanosarcinae and
563 description of Methanosarcina vacuolata sp. nova. *Microbiology* **48:** 279-285.
564 Zhilina, T.N. and G.A. Zavarzin. 1987. *Methanosarcina vacuolata* sp. nov., a vacuolated
565 Methanosarcina. *Int. J. Syst. Bacteriol.* **37:** 281-283.
566

**Table 1.** Comparison of Genome Features Among *Methanosarcina* spp.

| **Organism** | *Methanosarcina acetivorans* | *Methanosarcina mazei* | *Methanosarcina barkeri fusaro* | *Methanosarcina barkeri fusaro* | *Methanosarcina barkeri fusaro* |
|---|---|---|---|---|---|
| **tax_id** | 188937 | 192952 | 269797 | 269797 | 269797 |
| **Accession** | NC_003552 | NC_003901 | NC_007355 | NC_007349 | |
| **designation** | chromosome | chromosome | chromosome | plasmid | genome |
| **length** | 5751494 | 4096345 | 4837408 | 36358 | 4873766 |
| **G+C%** | 42.7% | 41.5% | 39.2% | 33.6% | 39.2% |
| **feature count** | 4540 | 3371 | 3680 | 18 | 3698 |
| **features length** | 4262934 | 3074712 | 3390164 | 21099 | 3411263 |
| **features coverage** | 74% | 75% | 70% | 58% | 69% |
| **featureless** | 26% | 25% | 30% | 42% | 31% |
| **nt/feature mean** | 939 | 912 | 921 | 1172 | 922 |

573 **Table 2.** Intergenomic distances calculated using eq 1 based on whole genome
574 maximal local nucleotide sequence identity considering only HSPs with identity > 67%
575 (lower left) or 55% (upper right).

576

| | ***M. acetivorans*** | ***M. mazei*** | ***M. barkeri*** | ***M. barkeri* plasmid** |
|---|---|---|---|---|
| ***M. acetivorans*** | 0 | 0.489 | 0.487 | 0.570 |
| ***M. mazei*** | 0.517 | 0 | 0.480 | 0.591 |
| ***M. barkeri*** | 0.552 | 0.569 | 0 | 0.512 |
| ***M. barkeri* plasmid** | 0.881 | 0.883 | 0.836 | 0 |

577

578

579 **Table 3.** Identification of conserved features for chromosomal origins of replication in
580 *Methanosarcina* spp.
581
582
583

| Description | strand | *M. acetivorans* | *M. barkeri* | *M. mazei* |
|---|---|---|---|---|
| conserved hypothetical | + | GI:20093437 | GI:73668510 | GI:21227413 |
| conserved hypothetical | + | GI:20093438 | GI:73668511 | GI:21227414 |
| conserved hypothetical | + | GI:20093439 | GI:73668512 | GI:21227415 |
| orc1 A | - | GI:20088900 | GI:73668513 | GI:21227416 |
| ORI A | | 1529 - 3357 | 1189197 - 1191361 | 1564667 - 1566241 |
| inter-origin region | variable | ~100Kbp | ~300Kbp | ~100Kbp |
| conserved hypothetical | - | GI:20088912 | GI:73668731 | GI:21227479 |
| ORI B | | 104571 - 105272 | 1481179 - 1482170 | 1654267 - 1655075 |
| orc1 B | + | GI:20088912 | GI:73668732 | GI:21227480 |
| Hsp60 | - | GI:20088912 | GI:73668733 | GI:21227481 |

584

# FIGURE LEGENDS

**Figure 1.** Thin-section electron micrograph of *M. barkeri* Fusaro showing typical morphology consisting of multicellular aggregates embedded in a methanochondroitin matrix. Vacuole-like structures appear to be membrane bound. Bars: A, 1.0 μm, B, 0.2 μm.

**Figure 2.** GRIT database schema. Primary keys are capitalized, foreign keys are underlined. Arrows indicate foreign key primary key relationships

**Figure 3.** The *M. barkeri* ORI A self-complementary region blastn alignment.

**Figure 4.** Asymmetric fragmentation in *M. barkeri*. The top panel shows cumulative deviations from the mean in *M. barkeri* genome for synteny (SI) with respect to *M. acetivorans* (a), *M. mazei* (b), or intergenic interval (c). The cumulative transposon count is superimposed (d). The bottom panel shows uniformly scaled blastn cross plots of *M. barkeri* chromosome with *M. mazei* and *M. acetivorans* with the origin regions circled.

**Figure 5.** Proposed mechanism for conserved repetitive sequence to provide bubbled-out repeat motifs for initiation of replication. Pairs of quasi-stable bubbles might occur in pairs at arbitrary locations on opposite strands. All motifs are essentially identical.

**Figure 6**. *M. acetivorans* is elongated due to distributed gene duplication events.

609 **Figure 1.** Thin-section electron micrograph of *M. barkeri* Fusaro showing typical
610 morphology consisting of multicellular aggregates embedded in a methanochondroitin
611 matrix. Vacuole-like structures appear to be membrane bound. Bars: A, 1.0 μm, B, 0.2
612 μm.

613

614

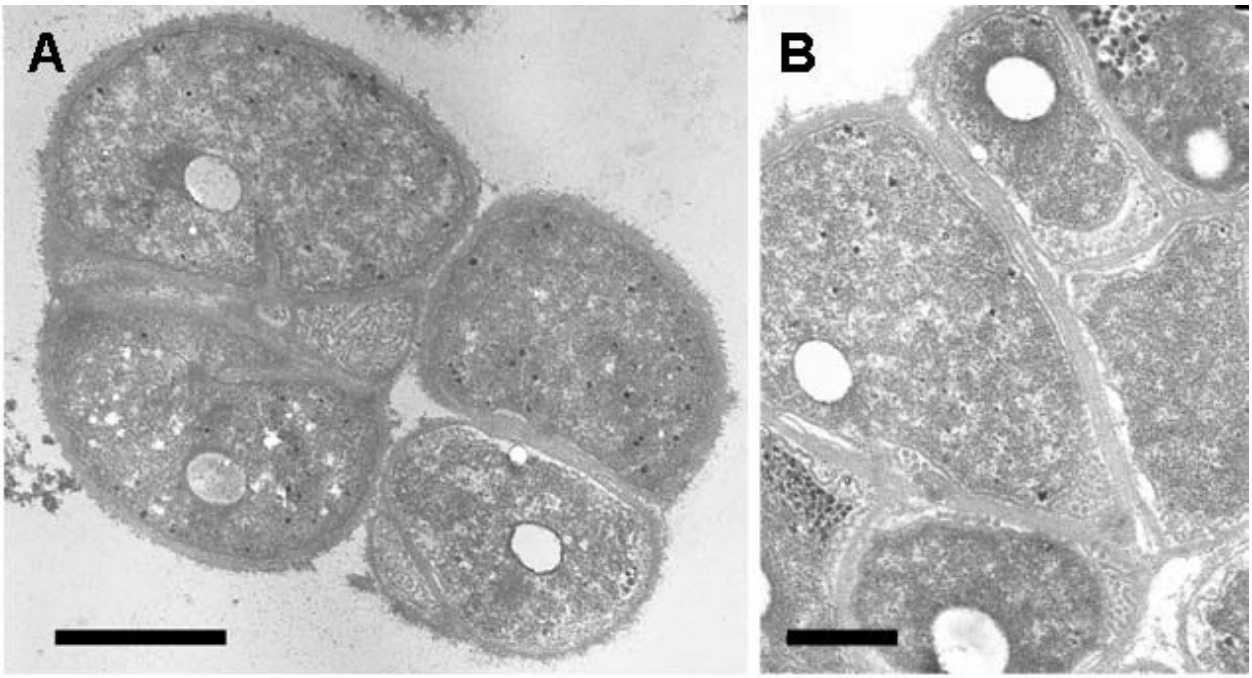


615

616

617

618

619

**Figure 2.** GRIT database schema. Primary keys are capitalized, foreign keys are underlined. Arrows indicate foreign key primary key relationships.

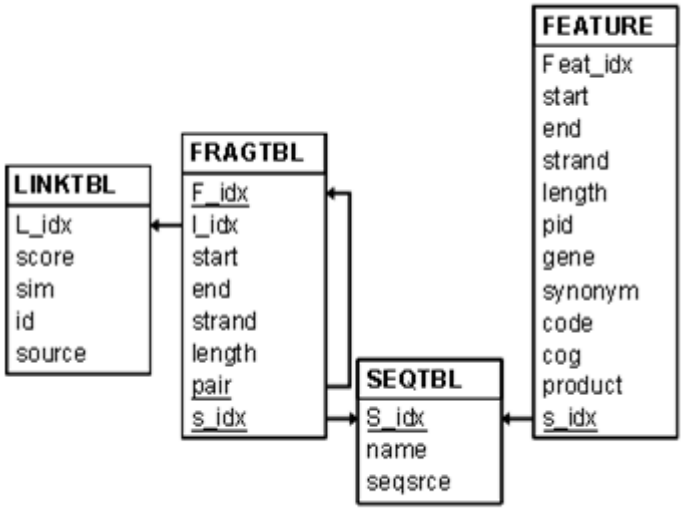


.

**Figure 3.** The *M. barkeri* ORI A self-complementary region blastn alignment

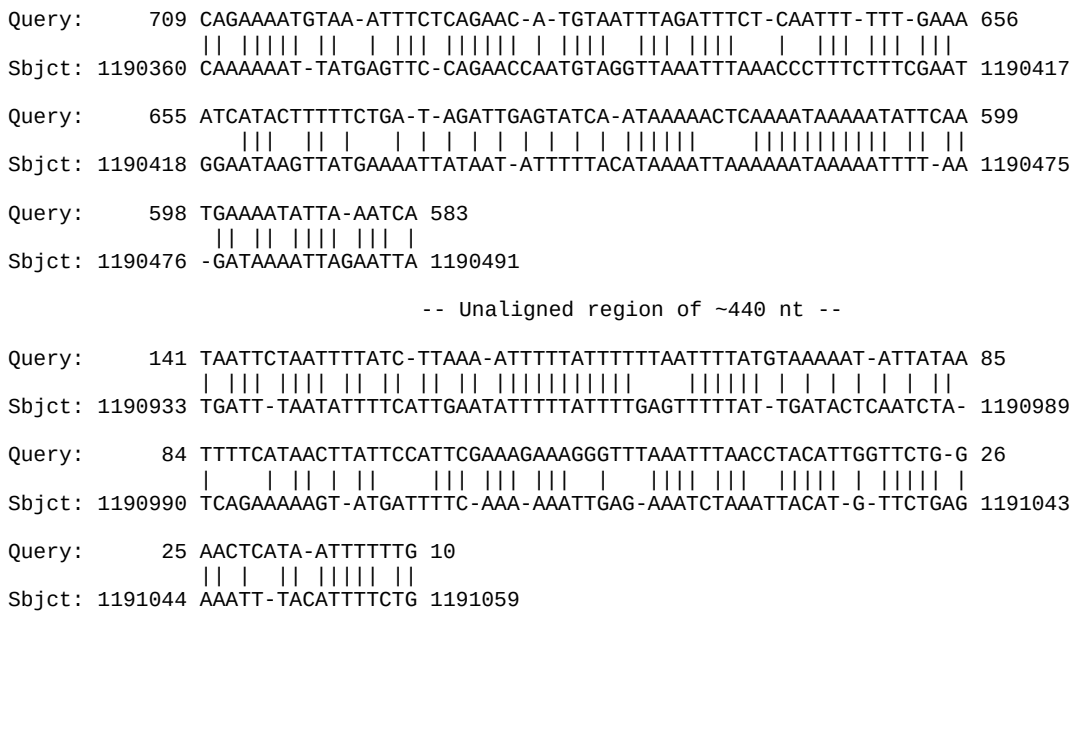

**Figure 4.** Asymmetric fragmentation in *M. barkeri*. The top panel shows cumulative deviations from the mean in *M. barkeri* genome for synteny (SI) with respect to *M. acetivorans* (a), *M. mazei* (b), or intergenic interval (c). The cumulative transposon count is superimposed (d). The bottom panel shows uniformly scaled blastn cross plots of *M. barkeri* chromosome with *M. mazei* and *M. acetivorans* with the origin regions circled.

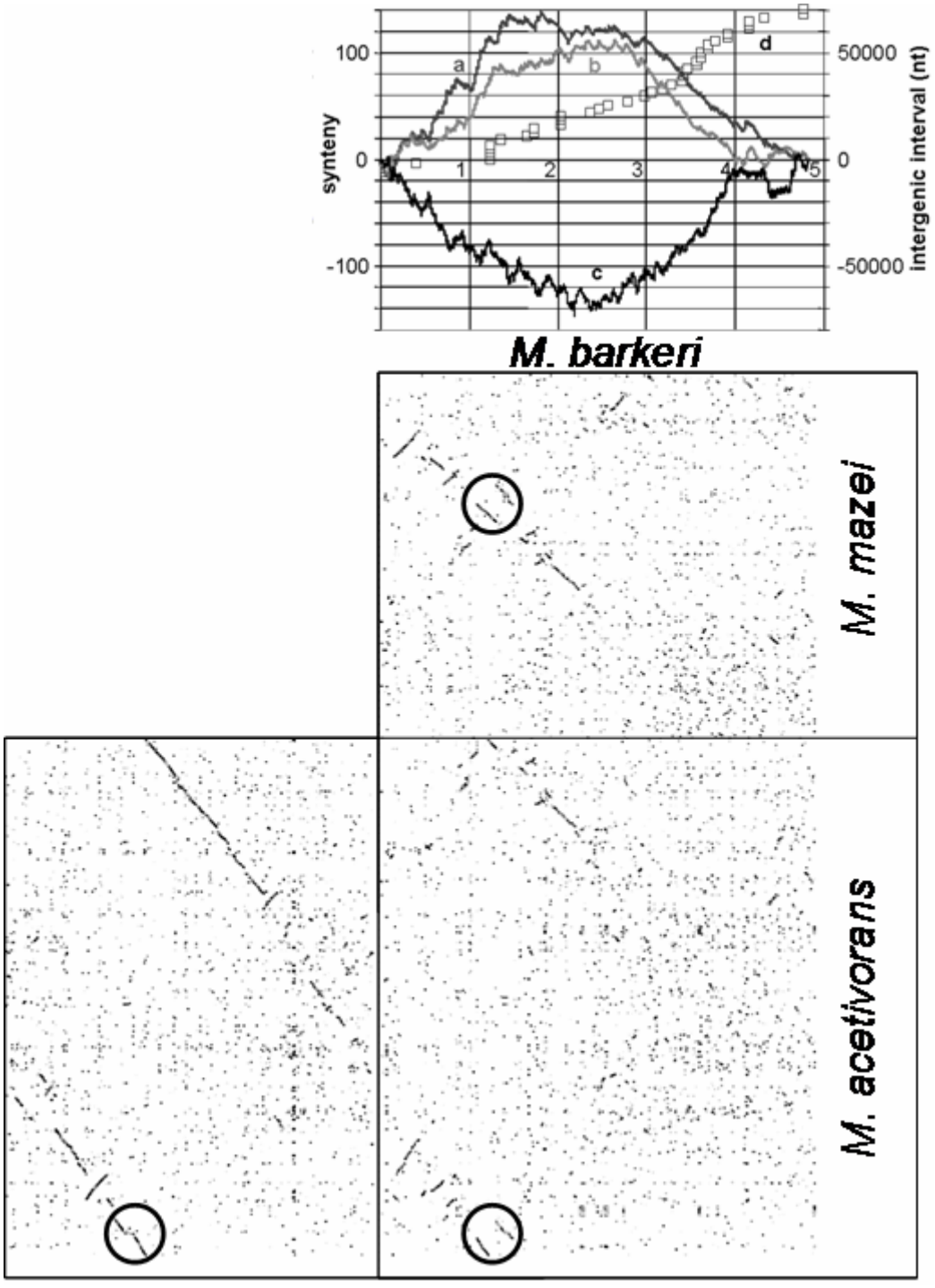

680
681
682 **Figure 5.** Proposed mechanism for conserved repetitive sequence to provide bubbled-
683 out repeat motifs for initiation of replication. Pairs of quasi-stable bubbles might occur in
684 pairs at arbitrary locations on opposite strands. All motifs are nearly identical.
685
686
687

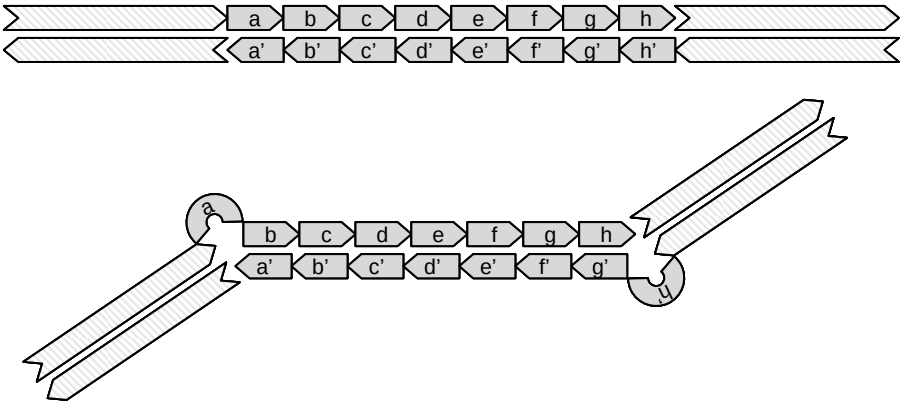

688 **Figure 6**. *M. acetivorans* is elongated due to distributed gene duplication events.
689
690
692
694

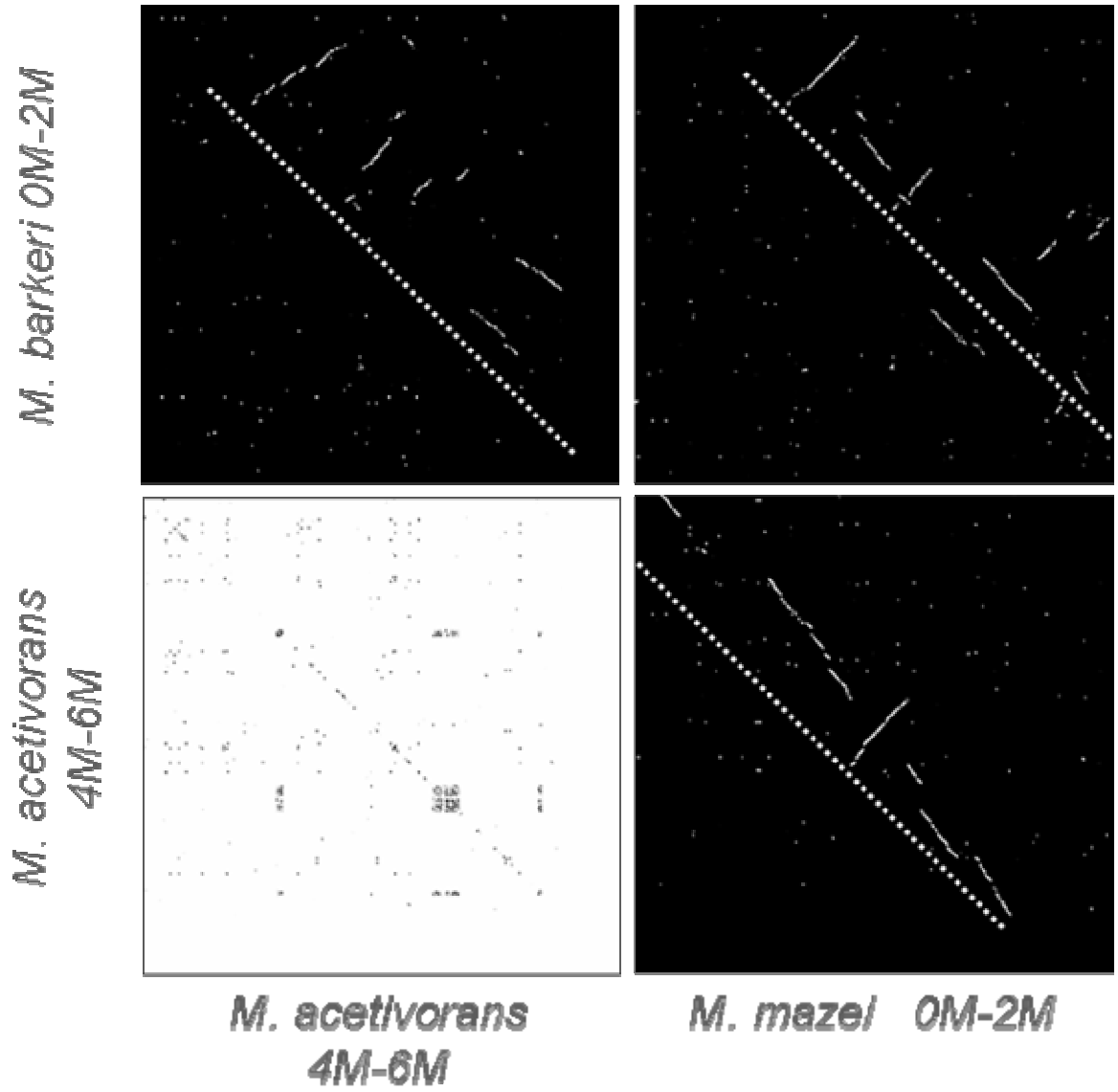

# SUPPLEMENT

**Figure S-1.** Plasmid DNA origin of replication containing a 5.6 kb non-coding region characterized by highly repetitive sequence consisting of over 38 direct repeats of a 143nt sequence with few variations between them.